

See discussions, stats, and author profiles for this publication at: <https://www.researchgate.net/publication/238126612>

Structural Modulation and Properties of Silver(I) Coordination Frameworks with Benzenedicarboxyl Tectons and trans -1-(2-Pyridyl)-2-(4-pyridyl)ethylene Spacer

ARTICLE *in* CRYSTAL GROWTH & DESIGN · APRIL 2010

Impact Factor: 4.89 · DOI: 10.1021/cg901188g

CITATIONS

46

READS

23

4 AUTHORS, INCLUDING:



Jing Chen

35 PUBLICATIONS 293 CITATIONS

[SEE PROFILE](#)



Miao Du

Tianjin Normal University

307 PUBLICATIONS 9,097 CITATIONS

[SEE PROFILE](#)

Structural Modulation and Properties of Silver(I) Coordination Frameworks with Benzenedicarboxyl Tectons and *trans*-1-(2-Pyridyl)-2-(4-pyridyl)ethylene Spacer

Cheng-Peng Li, Jing Chen, Qian Yu, and Miao Du*

College of Chemistry and Life Science, Tianjin Key Laboratory of Structure and Performance for Functional Molecule, Tianjin Normal University, Tianjin 300387, P. R. China

Received September 27, 2009; Revised Manuscript Received February 8, 2010

ABSTRACT: A series of silver(I) coordination polymers have been synthesized by the combination of an extended 2,4'-bipyridyl linker *trans*-1-(2-pyridyl)-2-(4-pyridyl)ethylene (bpe) and different benzenedicarboxyl tectons, including isophthalic acid (H_2ip), 5-sulfoisophthalic acid (H_3sip), terephthalic acid (H_2tp), 2-aminoterephthalic acid (H_2ata), and 2-bromoterephthalic acid (H_2bta). Single-crystal X-ray diffraction indicates that the structural patterns of these polymeric complexes diversify from two-dimensional (2-D) (3,4,5)-connected (for **2**) or 6^3 (for **3** and **4**) layers to three-dimensional (3-D) (10,3)-*b* (for **1**) or 8-nodal self-penetrating (for **5**) networks. Interestingly, the Ag^I centers can show various coordination spheres such as linear, trigonal, tetrahedral, and square-pyramidal geometries. The results clearly reveal that the dicarboxyl building blocks with different dispositions of the carboxyl sites and uncoordinated substituent groups, are the crucial factors for structural assemblies of such extended frameworks. Solid-state properties for these crystalline materials have also been investigated, which display modest thermal stability and strong fluorescent emission at room temperature.

Introduction

The significance of the investigation of crystal engineering of silver(I) coordination polymers lies in not only the fascinating activity of silver(I) for assembling unusual structural patterns,^{1,2} but also their relevance to a wide range of potential applications in the aspects of gas storage,³ antimicrobial,⁴ optical or electrical conductivity,⁵ catalysis,⁶ and even magnetic materials.⁷ In fact, the coordination sphere of silver(I) is readily adaptable to display variable stereochemical preferences and coordination numbers (normally ranging from two to six), which make it an appealing candidate for constructing diverse coordination networks.^{8–12} Thus, one major challenge faced in the design of such crystalline materials is to properly manipulate the coordination-driven assembly by using different organic ligands as structural-directed tectons. On the other hand, the geometrical flexibility of silver(I) also offers an opportunity to explore the inherent influence of the ligand functionality on forming the resulting coordination architectures. In this context, a variety of organic ligands containing different backbones and functional groups have been used to assemble one-, two-, and three-dimensional (1-D, 2-D, and 3-D) silver(I) coordination motifs.^{1–12} However, the effect of coordination-unfavored substituent groups for the bridging ligands on the formation of silver(I) coordination polymers has scarcely been demonstrated so far.¹³

Recently, we have employed some derivatives of the familiar building blocks isophthalate and terephthalate, which contain coordination-inert groups (such as $-NO_2$, $-OH$, $-SO_3H$, $-Br$, etc.^{14,15a,b}), to design new coordination polymers. In conjunction with different metal ions and/or dipyridyl-type coligands, various coordination motifs have been achieved, and the results clearly indicate the significant substituent effect on their structural assembly. In addition, we have also

investigated the role of a versatile supramolecular tecton, *trans*-1-(2-pyridyl)-2-(4-pyridyl)ethylene (bpe), on constructing coordination crystalline architectures.¹⁵ In general, this ligand can be considered as a bifunctional building block, in which the 4-pyridyl and 2-pyridyl groups are normally involved in coordinative and hydrogen-bonding interactions, respectively, in the resulting structural motifs due to their different steric hindrance. In this contribution, we select silver(I), bpe, and a series of related dicarboxyl coligands to prepare five novel polymeric complexes, namely, $[Ag(ip)_{1/2}(bpe)]_n$ (**1**), $\{[Ag_3(sip)(bpe)_2(H_2O)](H_2O)\}_n$ (**2**), $[Ag(tp)_{1/2}(bpe)]_n$ (**3**), $[Ag(ata)_{1/2}(bpe)]_n$ (**4**), and $\{[Ag_6(bta)_2(bpe)_4(NO_3)_2(H_2O)](H_2O)_2\}_n$ (**5**) (*ip* = isophthalate, *sip* = isophthalate-5-sulfonate, *tp* = terephthalate, *ata* = 2-aminoterephthalate, and *bta* = 2-bromoterephthalate). These coordination polymers show various 2-D and 3-D network architectures, which are regulated by the dicarboxyl ligands with dissimilar bridging backbones (angular or linear) and substituents as well as the sensitive coordination geometries of silver. Notably, the bpe ligand uniformly serves as the bridging spacer in complexes **1–5** that is quite unusual in other known examples.^{15b} In addition, thermal stability and solid-state fluorescent properties of these crystalline materials have also been explored.

Experimental Section

Materials and General Methods. All reagents and solvents were commercially available and used as received. Elemental analyses were carried out on a CE-440 (Leemanlabs) analyzer. Fourier transform (FT) IR spectra (KBr pellets) were taken on an AVATAR-370 (Nicolet) spectrometer. Thermogravimetric (TG) and differential thermal analysis (DTA) experiments were performed on a simultaneous TG-DTA system (Rigaku) in the temperature range of 25–600 °C under N_2 atmosphere (heating rate: 10 °C/min), in which an empty Al_2O_3 crucible was used as the reference. Powder X-ray diffraction (PXRD) patterns were recorded on a Shimadzu Maxima XRD-7000 diffractometer at 30 kV and 100 mA for a Cu-target tube ($\lambda = 1.5406 \text{ \AA}$), with a scan speed of 2°/min and a

*Corresponding author. E-mail: dumiao@public.tpt.tj.cn. Tel. and Fax: 86-22-23766556.

Table 1. Crystallographic Data and Structural Refinement Summary for Complexes **1–5**

	1	2	3	4	5
chemical formula	C ₁₆ H ₁₂ AgN ₂ O ₂	C ₃₂ H ₂₇ Ag ₃ N ₄ O ₉ S	C ₁₆ H ₁₂ AgN ₂ O ₂	C ₁₆ H ₁₃ AgN ₃ O ₂	C ₆₄ H ₅₂ Ag ₆ N ₁₀ O ₁₇ Br ₂
fw	372.15	967.25	372.15	387.16	2040.20
crystal size (mm ³)	0.24 × 0.22 × 0.16	0.24 × 0.23 × 0.22	0.24 × 0.22 × 0.18	0.24 × 0.20 × 0.18	0.24 × 0.22 × 0.16
crystal system	orthorhombic	triclinic	monoclinic	monoclinic	triclinic
space group	<i>Fdd2</i>	<i>P\bar{1}</i>	<i>P2₁/c</i>	<i>P2₁/c</i>	<i>P\bar{1}</i>
<i>a</i> (Å)	19.71(2)	9.7083(5)	7.1184(7)	7.203(3)	10.6107(4)
<i>b</i> (Å)	38.57(3)	10.2037(6)	19.046(2)	19.175(7)	17.4900(6)
<i>c</i> (Å)	7.082(5)	18.385(1)	10.0194(9)	10.141(4)	18.1407(6)
α (deg)	90	87.681(1)	90	90	94.227(1)
β (deg)	90	86.044(1)	106.237(1)	106.756(7)	97.312(1)
γ (deg)	90	63.827(1)	90	90	90.709(1)
<i>V</i> (Å ³)	5385(7)	1630.5(2)	1304.2(2)	1341.2(9)	3329.3(2)
<i>Z</i>	16	2	4	4	2
ρ_{calcd} (g/cm ³)	1.836	1.970	1.895	1.917	2.035
μ (mm ⁻¹)	1.502	1.910	1.551	1.514	3.008
<i>F</i> (000)	2960	952	740	772	1988
total/independent reflns	6597/1813	8298/5689	7023/2302	6779/2378	17298/11727
parameters	191	442	190	199	892
<i>R</i> _{int}	0.0303	0.0122	0.0235	0.0228	0.0225
<i>R</i> ^a , <i>R</i> _w ^b	0.0231, 0.0536	0.0274, 0.0608	0.0222, 0.0537	0.0346, 0.0968	0.0382, 0.0909
GOF ^c	1.070	1.039	1.043	1.084	1.049
residuals (e Å ⁻³)	0.401, -0.347	1.107, -0.853	0.415, -0.447	0.746, -0.888	1.065, -0.775

^a $R = \Sigma ||F_o| - |F_c|| / \Sigma |F_o|$. ^b $R_w = [\Sigma w(F_o^2 - F_c^2)^2] / \Sigma w(F_o^2)^2]^{1/2}$. ^c GOF = $\{\Sigma [w(F_o^2 - F_c^2)^2] / (n - p)\}^{1/2}$.

step size of 0.02° in 2θ. The calculated PXRD patterns were obtained from the single crystal X-ray diffraction data by using the PLATON program. Fluorescence spectra of the solid samples were measured on a Cary Eclipse spectrophotofluorimeter (Varian) at room temperature.

Preparation of the Complexes. $[\text{Ag(ip)}_{1/2}(\text{bpe})]_n$ (**1**). A mixture of bpe (18.4 mg, 0.1 mmol) and H₂ip (16.6 mg, 0.1 mmol) in methanol (10 mL) was carefully layered onto a water solution (5 mL) of AgNO₃ (17.0 mg, 0.1 mmol) in a straight glass tube, which was left to stand in darkness. Colorless block single crystals of **1** were obtained by slow evaporation of the solvent at room temperature after ca. 1 week. Yield: 23.1 mg (62%, based on bpe). Anal. Calcd for C₁₆H₁₂AgN₂O₂ (**1**): C, 51.64; H, 3.25; N, 7.53%. Found: C, 51.47; H, 3.09; N, 7.33%. IR (cm⁻¹): 1620 vs, 1555 s, 1472 m, 1391 s, 1221 w, 1154 w, 1064 w, 970 m, 877 w, 815 m, 742 m, 620 m, 542 m.

$[\text{Ag}(\text{sip})(\text{bpe})_2(\text{H}_2\text{O})](\text{H}_2\text{O})$ (**2**). The same synthetic method as that for **1** was used except that H₂ip was replaced by H₃sip (24.6 mg, 0.1 mmol). Colorless block crystals of **2** were obtained after ca. 5 days in 56% yield (18.1 mg, based on Ag^I). Anal. Calcd for C₃₂H₂₇Ag₃N₄O₉S (**2**): C, 39.74; H, 2.81; N, 5.79%. Found: C, 39.58; H, 2.89; N, 5.57%. IR (cm⁻¹): 3431 b, 1603 vs, 1556 s, 1471 w, 1425 m, 1363 s, 1194 s, 1100 m, 1043 m, 1005 w, 961 w, 871 w, 813 w, 770 m, 627 m, 541 m.

$[\text{Ag(tp)}_{1/2}(\text{bpe})]_n$ (**3**). The same synthetic procedure as that for **1** was used except that H₂ip was replaced by H₂tp (16.6 mg, 0.1 mmol), affording colorless block single crystals of **3** after ca. 1 week. Yield: 20.1 mg (54%, based on bpe). Anal. Calcd for C₁₆H₁₂AgN₂O₂ (**3**): C, 51.64; H, 3.25; N, 7.53%. Found: C, 51.77; H, 3.39; N, 7.41%. IR (cm⁻¹): 1684 w, 1570 vs, 1389 s, 1289 m, 1216 w, 1153 w, 1090 w, 997 w, 967 m, 881 w, 816 m, 742 m, 621 w, 543 m, 505 m.

$[\text{Ag(ata)}_{1/2}(\text{bpe})]_n$ (**4**). The same synthetic method as that for **1** was used except that H₂ip was replaced by H₂ata (18.1 mg, 0.1 mmol). Yellow block crystals of **4** were obtained after ca. 3 days in 66% yield (25.6 mg, based on bpe). Anal. Calcd for C₁₆H₁₃AgN₃O₂ (**4**): C, 49.64; H, 3.38; N, 10.85%. Found: C, 49.46; H, 3.55; N, 10.68%. IR (cm⁻¹): 3040 m, 1597 vs, 1558 vs, 1474 m, 1419 s, 1371 s, 1246 m, 1154 w, 1098 w, 968 w, 884 w, 816 m, 766 m, 630 w, 545 m.

$[\text{Ag(bta)}_2(\text{bpe})_4(\text{NO}_3)_2(\text{H}_2\text{O})](\text{H}_2\text{O})_2$ (**5**). The same synthetic method as that for **1** was used except that H₂ip was replaced by H₂bta (24.5 mg, 0.1 mmol), producing colorless block single crystals of **5** after ca. 1 week. Yield: 16.7 mg (49%, based on Ag^I). Anal. Calcd for C₆₄H₅₂Ag₆N₁₀O₁₇Br₂ (**5**): C, 37.68; H, 2.57; N, 6.87%. Found: C, 37.41; H, 2.47; N, 6.88%. IR (cm⁻¹): 3426 b, 1708 m, 1602 s, 1473 m, 1382 vs, 1233 m, 1157 w, 1090 w, 1056 w, 1007 w, 964 m, 879 w, 817 m, 767 m, 633 w, 543 m.

X-ray Crystallography. Single-crystal X-ray diffraction data for complexes **1–5** (CCDC reference numbers: 746674–746678) were collected on a Bruker Apex II CCD diffractometer with Mo Kα radiation ($\lambda = 0.71073$ Å) at room temperature. There was no evidence of crystal decay during data collection. In each case, a semiempirical absorption correction was applied (SADABS) and the program SAINT was used for integration of the diffraction profiles. All structures were solved by direct methods using SHELXS and refined with SHELXL. The non-hydrogen atoms were modeled with anisotropic displacement parameters and refined by full-matrix least-squares methods on F^2 . Generally, C-bound H atoms were placed geometrically and refined as riding, whereas O- and N-bound H atoms (for water molecules in **2** and **5**, and -NH₂ in **4**) were first determined in difference Fourier maps and then fixed in the calculated positions. Further crystallographic details are summarized in Table 1.

Results and Discussion

Synthesis and General Characterization. Coordination polymers **1–5** were synthesized via layer-separation diffusion method under ambient conditions, affording well-shaped X-ray qualified single crystals. In each case, an equimolar ratio of silver(I)/bpe/dicarboxyl was used for the starting reagent, and however, the stoichiometric composition was changed in the resulting crystalline product. All complexes are insoluble in common organic solvents and water, which were characterized by IR, microanalysis, and powder X-ray diffraction (PXRD). In the IR spectra of complexes **2** and **5**, the broad peaks at ca. 3400 cm⁻¹ indicate the presence of water molecules. The absence of characteristic absorption band of carboxyl (at ca. 1700 cm⁻¹) in the IR spectra of **1–5** confirms the complete deprotonation of the dicarboxyl ligand. The IR spectrum of **5** shows a sharp band with very strong intensity at 1382 cm⁻¹, revealing the existence of nitrate anion. In addition, the phase purity of the bulk samples for **1–5** was confirmed by PXRD patterns at room temperature, which agree well with the calculated ones (see Figure S1 in Supporting Information).

Structural Description of **1–5.** $[\text{Ag(ip)}_{1/2}(\text{bpe})]_n$ (**1**). Complex **1** represents a 3-D polymeric structure which crystallizes in the acentric space group *Fdd2* with the flack parameter being refined to near zero. The asymmetric unit contains one

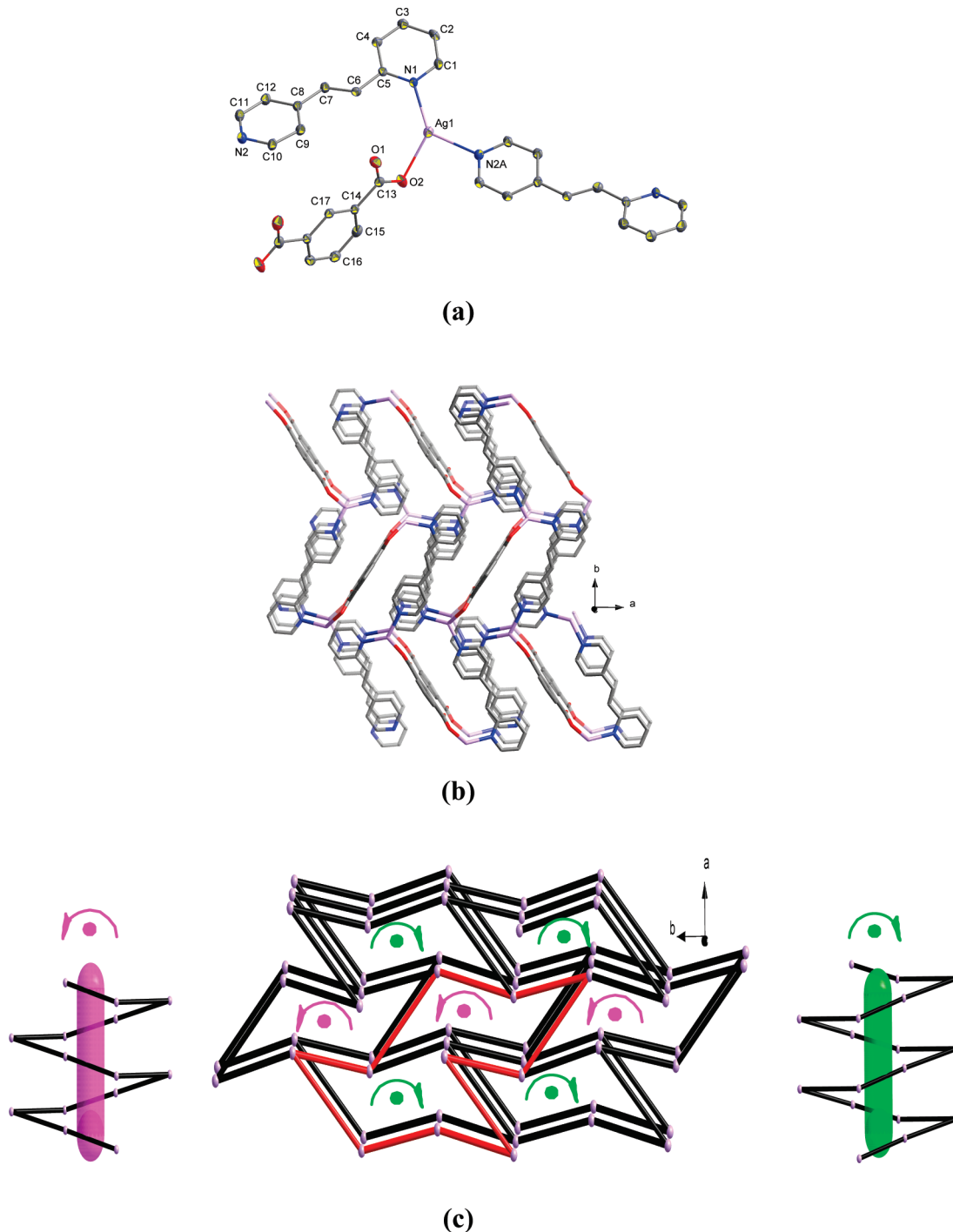


Figure 1. Views of **1**. (a) Coordination environment of Ag^{I} with ellipsoids drawn at the 30% probability level (symmetry code: $A = -x + 1/4$, $y + 1/4$, $z + 1/4$). (b) Perspective view of the 3-D coordination framework. (c) Schematic illustration of the $(10,3)$ - b network constructed via helical arrays along the c axis, in which the bpe and ip spacers are represented as the rods and one shortest 10-membered ring is highlighted in red.

Ag^{I} ion, one bpe, and one-half-occupied ip ligand with C_2 symmetry (see Figure 1a). The Ag^{I} center adopts a trigonal coordination geometry (see Table S1 for detailed bond parameters), ligating to two nitrogen atoms of 2- and 4-pyridyl rings from two bpe, and one carboxylate oxygen atom from ip, in which the Ag^{I} ion deviates from the least-squares basal plane by 0.270 Å. Both the ip and bpe ligands play the bridging role to link the Ag^{I} centers, and as a result, a 3-D polymeric coordination network is formed (see Figure 1b). In such a framework, 1-D hexagonal helical

arrays are observed along the c -axis, and notably, different left- and right-helices are arranged in an alternative fashion along the a -axis (see Figure 1c, pink and green arrows). Additionally, $\pi-\pi$ stacking interactions¹⁷ are found between the adjacent 2- and 4-pyridyl rings (dihedral angle = 7.3(1)°) of the bpe ligands, with the centroid-to-centroid distance of 3.957(4)/3.814(4) Å and the displacement angle (formed between the ring-centroid vector and the ring normal to one of the pyridyl planes) in the range of 23.3(1)–29.5(1)°. A further topological analysis of this 3-D architecture indicates

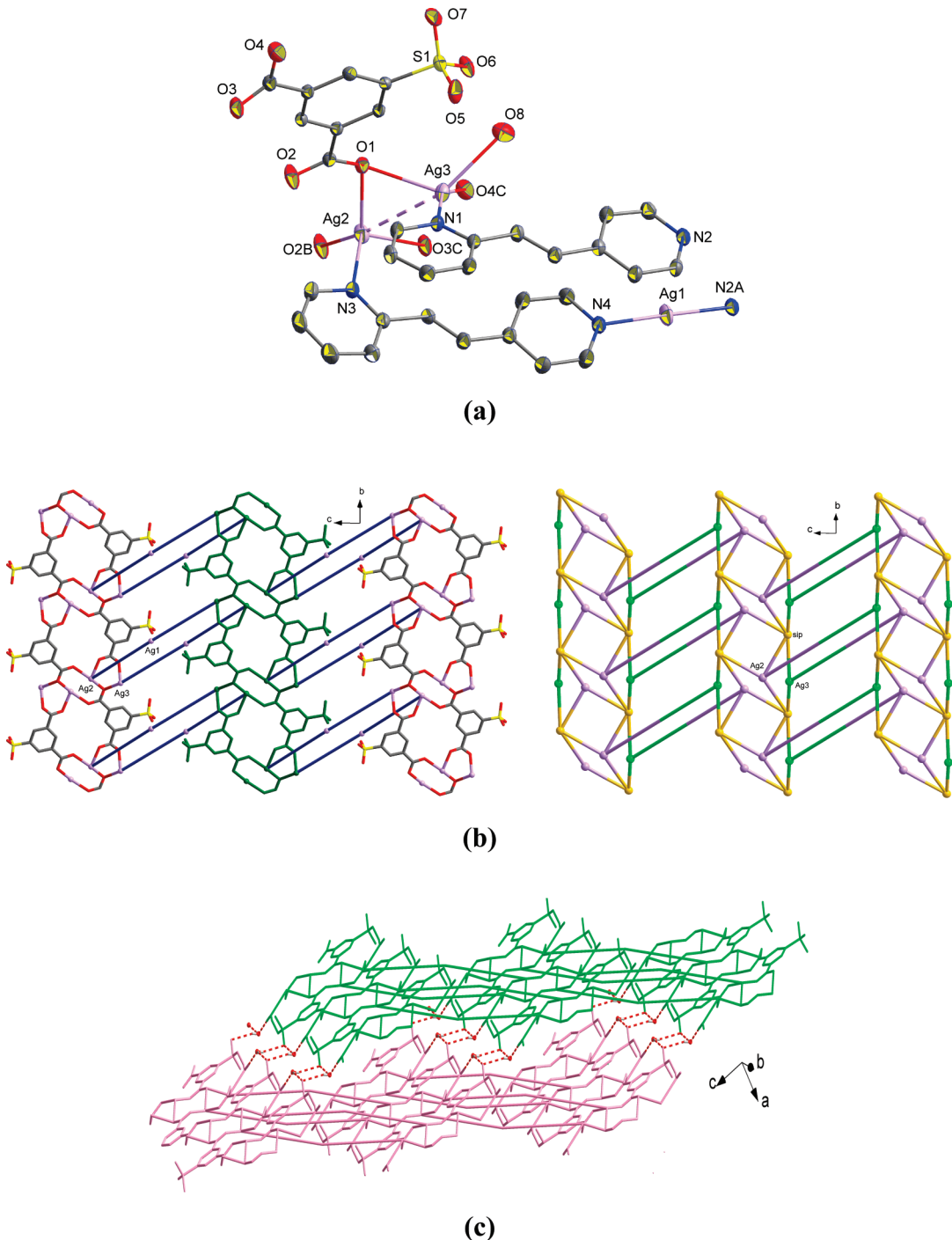


Figure 2. Views of **2**. (a) Coordination environments of the Ag^{I} centers with ellipsoids drawn at the 30% probability level (symmetry codes: A = $-x + 1, -y, -z + 2$; B = $-x + 2, -y + 1, -z + 1$; C = $x, y - 1, z$). (b) (left) Perspective view of the 2-D coordination layer (the bpe ligands are reduced to blue rods for clarity) and (right) schematic representation of the trinodal network. (c) 3-D supramolecular network showing the interlayer $\text{O}-\text{H}\cdots\text{O}$ hydrogen bonding (red dashed lines).

that the uniform 3-connected Ag^{I} nodes are extended by both ip and bpe spacers to result in a (10,3)-*b* network that is equivalent to the ThSi_2 (ths^{18}) lattice, in which the repeating subunit is composed of 10 silver centers that are bridged via six bpe and four ip connectors (see Figure 1c).

$\{[\text{Ag}_3(\text{sip})(\text{bpe})_2(\text{H}_2\text{O})](\text{H}_2\text{O})\}_n$ (**2**). The structure of **2** presents a layered coordination framework with a unique mixed-connected network topology. The asymmetric unit consists of three Ag^{I} ions, a pair of bpe, one sip trianion, and two coordinated/lattice water molecules. Interestingly, the

Ag^{I} centers take different coordination spheres (see Figure 2a). The $\text{Ag}1$ ion shows an approximately linear coordination geometry consisting of 4-pyridyl nitrogen atoms from two different bpe ligands. Both $\text{Ag}2$ and $\text{Ag}3$ exhibit the tetrahedral geometries, coordinating to three carboxylate oxygens from sip and one 2-pyridyl nitrogen from bpe for $\text{Ag}2$, and two carboxylate oxygens from sip, one 2-pyridyl nitrogen from bpe, and one aqua ligand for $\text{Ag}3$. Notably, the neighboring $\text{Ag}2\cdots\text{Ag}3$ separation is 3.118(1) Å, which is shorter than that of van der Waals $\text{Ag}\cdots\text{Ag}$

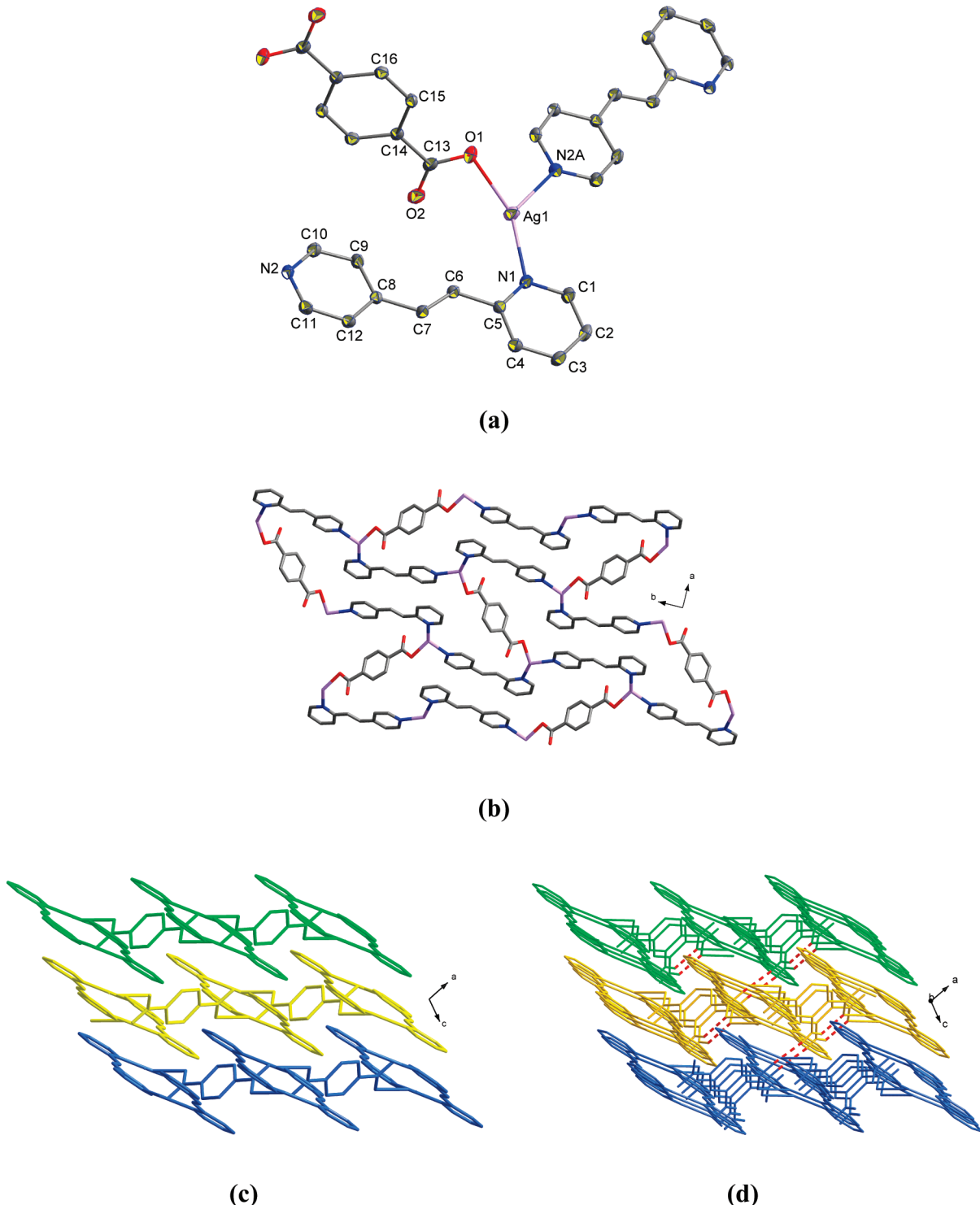


Figure 3. Views of **3** and **4**. (a) Coordination environment of Ag⁺ in **3** with ellipsoids drawn at the 30% probability level (symmetry code: A = $-x + 1, y + 1/2, -z + 1/2$). (b) Perspective view of the 2-D coordination layer in **3** with 6³ topology. (c) Packing diagram of **3**. (d) Packing diagram of **4** showing the intralayer and interlayer N-H···O hydrogen bonding (red dashed lines).

interaction (3.40 Å) and longer than that of metallic silver (2.89 Å), indicating the presence of argentophilic interactions.¹⁹ The two carboxylate groups of sip display the μ -O,O' and μ -O,O- μ -O,O' coordination fashions, respectively, and as a result, the Ag²⁺ and Ag³⁺ ions are linked by the sip bridges to afford a 1-D ladder-like coordination array along the [010] axis. In addition, such 1-D arrays are further extended by the [bpe-Ag¹⁺-bpe] rods to constitute a complicated 2-D architecture (see Figure 2b left). From the viewpoint of

topological analysis, each Ag²⁺, Ag³⁺, and sip can be considered as the four-, three-, and five-connected nodes, respectively, and each Ag¹⁺ and bpe as the two-connected spacers, leading to the generation of a trinodal network with the Schläfli symbol of (4.6²)(4³.6².8)(4⁴.6⁶), which represents a new type of 2-D topological structure (see Figure 2b right).²⁰ Furthermore, each lattice water molecule acts as a trifurcate bridging via H-bonding interactions (O8-H8B···O9, O9-H9A···O7, and O9-H9B···O7, see Table S2 for

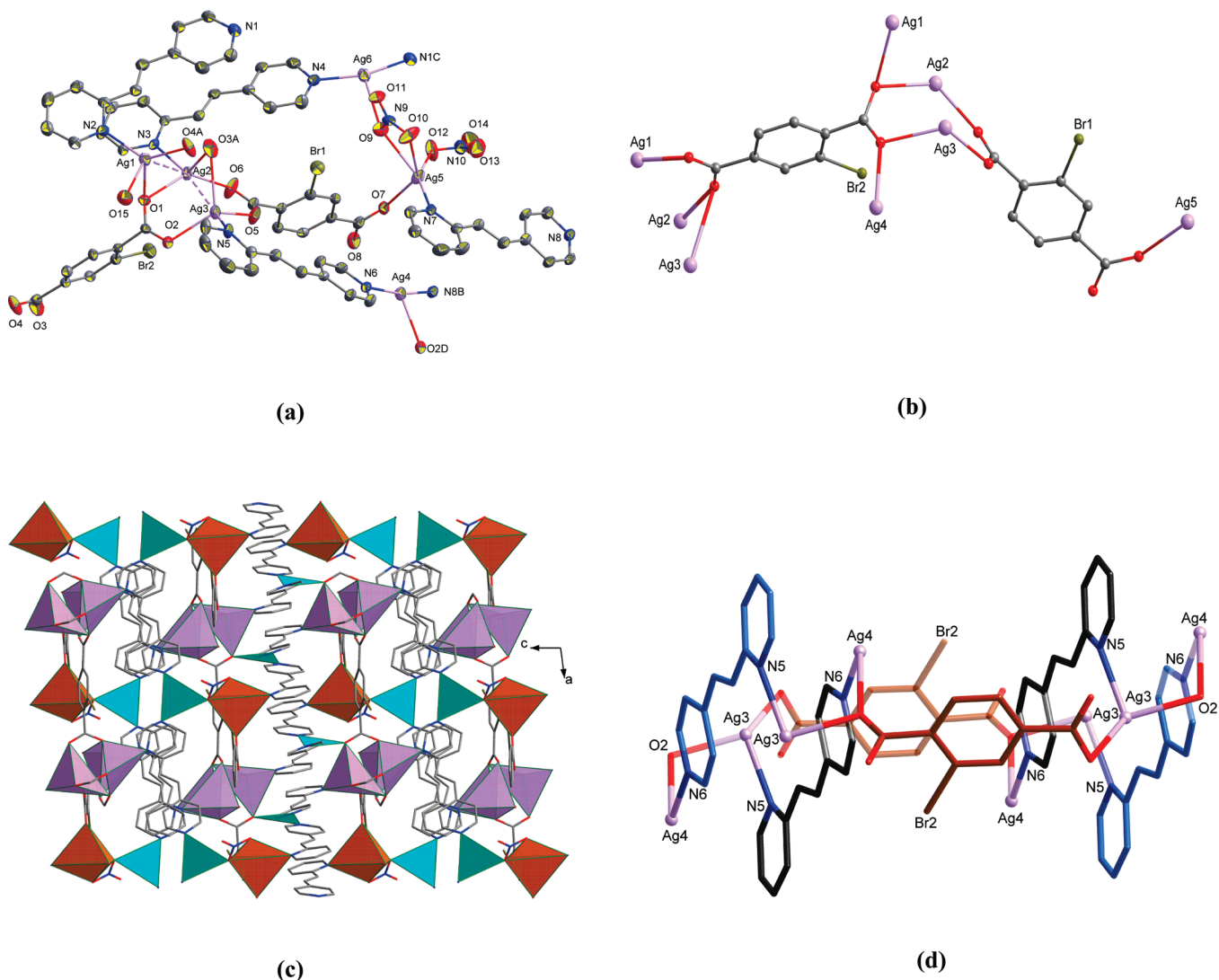


Figure 4. Views of **5**. (a) Coordination environments of the Ag^{I} centers with ellipsoids drawn at the 30% probability level (symmetry codes: A = $x - 1, y, z$; B = $-x + 1, -y - 1, -z + 1$; C = $-x + 1, -y, -z + 2$; D = $-x + 2, -y, -z + 1$). (b) Bridging fashions of the bta ligands. (c) Perspective view of the 3-D polymeric framework with the Ag^{I} ions shown in polyhedral modes (turquoise trigon for $\text{Ag}4/\text{Ag}6$, purple tetrahedron for $\text{Ag}1/\text{Ag}2/\text{Ag}3$, and brown square-pyramid for $\text{Ag}5$). (d) Schematic illustration of the self-penetrating supramolecular pattern.

details), connecting the adjacent 2-D arrays to result in a 3-D supramolecular network (see Figure 2c). Intramolecular O8–H8A···O6 interactions are also observed between the aqua ligands and sulfonate groups of sip within the 2-D layer. No π – π stacking interaction is found in this structure.

[Ag(tp)_{1/2}(bpe)]_n (**3**) and **[Ag(ata)_{1/2}(bpe)]_n** (**4**). Single-crystal X-ray diffraction analysis reveals that complexes **3** and **4** are isostructural, and thus herein, only the crystal structure of **3** is described in detail. The asymmetric unit of complex **3** consists of one Ag^{I} center, one bpe, and one-half-occupied ip anionic ligand lying about an inversion center (see Figure 3a). Similar to that in **1**, the Ag^{I} ion in **3** adopts a trigonal coordination geometry and deviates from the basal plane by 0.247 Å, which is provided by two pyridyl nitrogen donors from two bpe, and one carboxylate oxygen atom from tp. In this way, the Ag^{I} centers are extended by the tp and bpe spacers to result in a 2-D 6³ layer along the *ab* plane (see Figure 3b). These parallel 2-D layers show a close interdigitating stacking fashion along the *c* axis

(see Figure 3c). Interlayer π – π stacking interactions are observed between the 2- and 4-pyridyl rings (dihedral angle = 4.3(1)°) of bpe coming from the adjacent layers, with the centroid-to-centroid distance of 3.746(2) Å and the displacement angle of 25.0(1)/25.2(1)°. Comparable intra-layer π – π stacking interactions are also found, with the centroid-to-centroid distance of 3.949(2) Å, the dihedral angle of 4.3(1)°, and the displacement angle of 27.2(1)/31.1(1)°. No classical hydrogen-bonding interaction exists in this structure.

Notably, although complex **4** also shows a similar 2-D coordination layer, the presence of an amino group of ata leads to the formation of additional H-bonding interactions (see Table S2, Supporting Information for details). Besides intramolecular N3–N3B···O1 bonds, interlayer N3–N3A···O2 interactions further extend the 2-D layers to result in a 3-D supramolecular network (see Figure 3d). Similar to those in **3**, intra- and interlayer π – π stacking interactions are also observed in **4**, with the centroid-to-centroid distance of 3.964(3) and 3.693(3) Å, the dihedral

Table 2. A Comparison of the Structural Features for Complexes **1–5**

complex	silver(I) sphere	μ_N^a	coordination motif	$\text{Ag}\cdots\text{X}\cdots\text{Ag}$ (deg) ^b	$\text{Ag}\cdots\text{Ag}$ (Å) ^c	θ (deg) ^d
1 (ip)	trigonal	2	3-D (10,3)- <i>b</i> net	73.5(1)	9.918(7)	17.3(1)
2 (sip)	linear/tetrahedral	5	2-D 3-nodal layer	65.7(1)/68.7(1)	9.3838(6)/9.1950(6)	9.5(1)/16.1(1)
3 (tp)	trigonal	3	2-D 6 ³ layer	70.5(1)	9.6509(9)	4.3(1)
4 (ata)	trigonal	3	2-D 6 ³ layer	71.7(1)	9.768(4)	2.5(1)
5 (bta)	trigonal/tetrahedral/ square pyramidal	3/7	3-D 8-nodal net (self-penetrating)	66.3(1)/65.2(1)/ 70.3(1)/67.0(1)	9.2381(6)/9.2822(7)/ 9.1847(8)/9.2486(8)	10.2(2)/15.6(2)/ 4.4(2)/8.2(2)

^aThe number of silver(I) ions bridged by one benzenedicarboxylate ligand. ^bThe angle between the center of 2-pyridyl ring for one bpe ligand and two silver(I) centers bridged by it. ^cThe distance between two silver(I) centers bridged by one bpe ligand. ^dThe dihedral angle between two pyridyl rings within a bpe ligand.

angle of 2.4(1)°, and the displacement angle in the range of 22.8(1)–31.0(1)°.

$[\text{Ag}_6(\text{bta})_2(\text{bpe})_4(\text{NO}_3)_2(\text{H}_2\text{O})](\text{H}_2\text{O})_2\}_{n}$ (**5**). In the asymmetric unit of **5**, there exist six independent Ag¹ centers, two bta dianions, four bpe ligands, two nitrate anions, as well as one coordinated and two lattice water molecules. As depicted in Figure 4a, the coordination geometries of Ag1, Ag2, and Ag3 are similar, in which the distorted tetrahedron is defined by one nitrogen and three oxygen donors (bpe + 2bta + H₂O for Ag1 and bpe + 3bta for Ag2/Ag3). For Ag4 and Ag6, each Ag¹ ion is surrounded by one oxygen and two nitrogen atoms to feature a trigonal coordination geometry (2bpe + bta for Ag4 and 2bpe + nitrate for Ag6). In addition, Ag5 displays a five-coordinated distorted square pyramidal sphere with the τ parameter of 0.21,²¹ being completed by one nitrogen and four oxygen atoms (bpe + bta + 2nitrate). In this case, the two nitrate anions adopt the unidentate and μ -O,O- η -O,O' coordination modes, respectively. Notably, the two bta ligands are connected to three and seven Ag¹ centers, respectively, in which the carboxylate groups take the unidentate and μ -O,O' as well as μ -O,O- μ -O,O' and μ -O,O- μ -O,O'- μ -O,O' binding fashions (see Figure 4b). The nearest distances of Ag1…Ag2 and Ag2…Ag3 are 3.3501(7) and 2.8938(6) Å, indicating the argentophilic interactions. Because of the significant steric effect of 2-bromo substituent, its neighboring carboxylate group of bta is forced out of the central phenyl plane to take a nearly perpendicular disposition, with the dihedral angle of 69.2(2)° for O5—C57—O6 and 83.8(2)° for O1—C49—O2. As a result, a very complicated 3-D polymeric network is constructed by the combination of diverse Ag¹ ions and bta bridging ligands (see Figure 4c). In addition, multiple O—H…O interactions involving coordination/lattice water, carboxylate, and nitrate (see Table S2, Supporting Information for details) are also observed and no π — π stacking interaction exists in this structure.

In order to properly understand the structural assembly of this intricate 3-D network, the topological method is used to simplify the polymeric framework. In this case, Ag1, Ag4, Ag5, and Ag6 could be regarded as the three-connected nodes, with the vertex symbols of (4₂.84.84), (6₂.8.10₂), (4.8.10₅), and (4.8.8.10₁₈), respectively. Moreover, Ag2 and Ag3 serve as the four-connected nodes with the vertex symbols of (4.4₂.4.6.4.6) and (4.6.4.6.4₂.8₃), respectively. In addition, the two bta bridging ligands should be considered as the three- and seven-connected nodes (linking to Ag2 + Ag3 + Ag5 and 2Ag1 + 2Ag2 + 2Ag3 + Ag4) with the vertex symbols of (4.4₂.6₂) and (4.4.4.4₂.4₂.6.6.8.8.8.8₂.8₂.8₃.8₃.10₁₀.10₁₀.10₁₃.10₁₃), respectively. As a result, this 3-D coordination framework represents a 8-nodal mixed-connected network with the Schläfli symbol of (4.8.10)₂-(4.8²)(4².6)(4³.6².8)(4⁴.6²)(4⁶.6².8⁹.10⁴)(6.8.10). Significantly,

this unique network also displays a self-penetrating supramolecular prototype, in which one of the shortest circuits consisting of Ag3, Ag4, bpe, and bta components is penetrated by a pair of bpe spacers (see Figure 4d).

Structural Features for Coordination Networks of **1–5**.

From the above description, the bpe ligands uniformly behave as the bidentate spacers to connect the Ag¹ centers in the resulting networks of **1–5**, and thus, their structural discrepancy should be mainly attributed to the choice of different benzenedicarboxyl tectons. A comprehensive comparison of the structural features for these polymeric complexes is listed in Table 2. Notably, in most of the known examples, bpe normally serves as the unidentate terminal around the metal center.¹⁵ In this study, the bpe spacer bridges the Ag¹ ions with the Ag…X…Ag (X is centroid of the 2-pyridyl group) angles in the range of 65.2(1)–73.5(1)° (see Table 2), which are comparable to those observed for the reported structures, such as 59.6(1)/58.5(1)° in [Ag_n(bpe)(NO₃)_n],^{22a} 66.7(1)/69.1(1)° in {[Cu¹(bpe)]_n(BF₄)_n},^{22b} 68.1(1)° in {[Cd(bpe)(tp)(H₂O)](H₂O)_n}, 67.6(1)/63.8(1)° in {[Cd₂(bpe)₂(hip)₂(CH₃OH)(H₂O)](H₂O)₄}_n (hip = 5-hydroxylisophthalate), and 66.5(1)/67.0(1)° in {[Cd₂(bpe)₂(ip)₂(CH₃OH)(H₂O)](H₂O)₄}_n.^{15b} Additionally, the distances of Ag…Ag separated by a bpe ligand are ca. 9.2–9.9 Å in **1–5** (see Table 2), and the corresponding values in the above-reported examples are 8.758(2)/8.848(2), 9.1555(8)/9.0699(8), 9.550(2), 9.4927(4)/9.2232(5), and 9.4233(8)/9.407(1) Å, respectively. The modest variety of such structural parameters corresponds to different degrees of distortion of the pyridyl groups in bpe (see Table 2 for the dihedral angles²³) and also reveals some flexibility of such a tecton in coordination assembly for properly meeting the steric requirement. Notably, the nearest centroid-to-centroid distance between two olefin bonds of adjacent bpe ligands in **1**, **3**, and **4** is within 4.2 Å (ca. 3.93 Å for **1**, 4.21 Å for **2**, 3.99 Å for **3**, 4.01 Å for **4**, and 4.48 Å for **5**), indicating the possibility of a topochemical [2 + 2] cycloaddition reaction.²⁴

As a result, the dicarboxylate building blocks varied in the assembled process are capable of diversifying the structural extension of coordination networks for **1–5** by using different bridging fashions. For example, with regard to **1** and **2**, the angular ligands H₂ip and H₃sip are fully deprotonated to coordinate with silver(I) in a 1:2 or 1:3 stoichiometric ratio, and the binding fashions of carboxylate groups vary from unidentate for **1** to μ_2/μ_3 -bridging for **2**. Correspondingly, their network structures are changed from a 3-D (10,3)-*b* framework to a 2-D (3,4,5)-connected layer. When the linear dicarboxyl H₂tp and its derivatives H₂ata and H₂bta are used, the 2-D 6³ coordination layers (for **3** and **4**) and a very complicated 3-D 8-nodal network with the self-penetrating nature (for **5**) are constructed. As for the isostructural 2-D motifs of **3** and **4** (tp²⁻/ata²⁻:silver(I) = 1:2), the adding

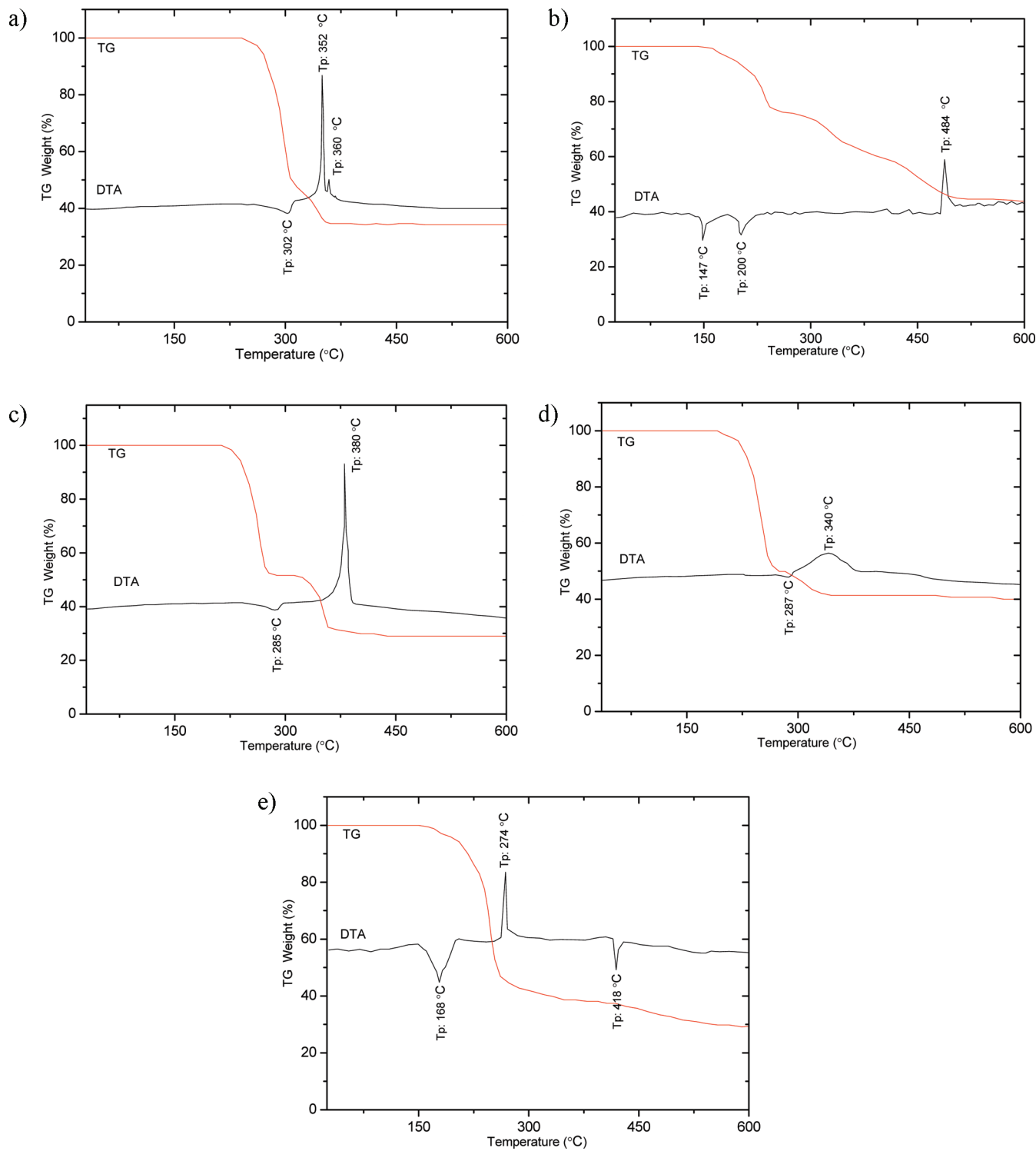


Figure 5. TG-DTA curves for complexes **1–5** (a–e).

of -NH_2 group in ata of **4** will not influence the basic coordination pattern, which however leads to the formation of expected H-bonding for further extension of the 2-D layers. Significantly, the steric effect of the -Br group in bta of **5** ($\text{bta}^{2-}:\text{silver(I)} = 1:3$) leads to rotation of the adjacent carboxylate around the aromatic plane, which allows the formation of dimeric $[\text{Ag}(\text{COO})_2]$ subunits and further results in a distinct and intricate 3-D framework, in which six types of Ag^{I} centers with diverse coordination spheres and two bta $^{2-}$ ligands with μ_3 - and μ_7 -bridging modes are

observed. In a word, the benzenedicarboxylate bridging ligands used in this work can serve as the versatile 2-, 3-, 5- and 7-connecting modules, which will be responsible for structural diversity of the resulting coordination frameworks, in combination with the adaptable configuration of Ag^{I} (linear, trigonal, tetrahedral, or square-pyramidal geometry).

Thermal Stability. Thermal properties of coordination polymers **1–5** were investigated by TG-DTA and in situ temperature-dependent PXRD techniques (see Figure 5 and

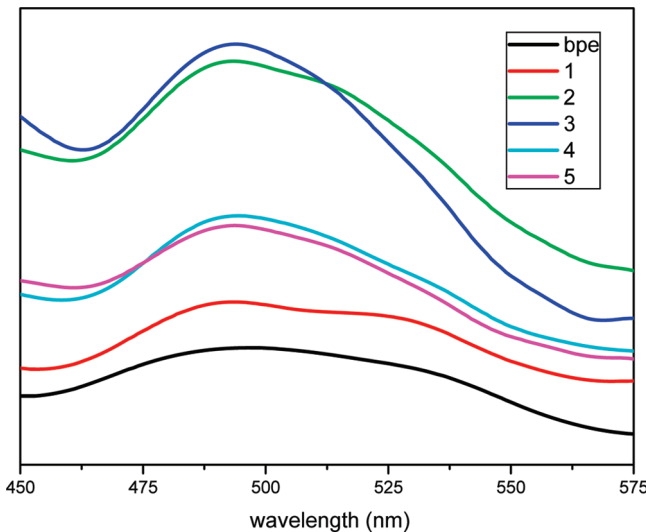


Figure 6. Solid-state fluorescent emission spectra for bpe and complexes **1–5**.

Figure S2 for TG-DTA curves and PXRD patterns, respectively). Complex **1** remains intact until heating to 241 °C, and then suffers several steps of weight loss that ends at 489 °C (one endothermic peak at 302 °C and two exothermic peaks at 352 and 360 °C in the DTA curve). Correspondingly, the in situ PXRD patterns are almost unchanged from room temperature to 200 °C and confirm the framework integrality. Further heating to 600 °C reveals no weight loss and the final solid holds a weight of 34.20% of the total sample. The TG curve of **2** shows the first weight loss of 3.83% in the temperature range of 141–183 °C, which indicates the exclusion of lattice and coordination aqua molecules (calculated: 3.73%). With that, pyrolysis of the residual component occurs and the final residue has a weight of 43.83% of the total sample. Accordingly, two endothermic peaks at 147 and 200 °C as well as one exothermic peak at 484 °C are observed in DTA. The PXRD patterns indicate that the coordination framework of **2** collapses above 200 °C after removing the aqua molecules. Complex **3** is thermally stable upon heating to 213 °C, followed by a sharp weight loss that ends at 288 °C, with one endothermic peak at 285 °C in DTA. After a short-lived stabilization, a gradual weight loss starts at 312 °C and ends at 535 °C, with one exothermic peak at 380 °C in DTA. Upon further heating to 600 °C, no weight loss is found and the final solid holds a weight of 29.02% of the total sample. With regard to **4**, pyrolysis of the polymeric framework occurs at 210 °C and ends at 577 °C, with one endothermic peak at 287 °C and one exothermic peak at 340 °C in the DTA curve. Further heating to 600 °C reveals no weight loss and the residue holds a weight of 39.97% of the total sample. For complexes **3** and **4**, the PXRD patterns indicate their framework stability upon heating to 200 °C. As for **5**, the first weight loss of 2.89% in the TG curve (150–181 °C) suggests the release of lattice and coordination aqua molecules (calculated: 2.65%). Subsequently, decomposition of the residual framework is observed, which does not end until heating to 600 °C. The corresponding DTA curve indicates two exothermic and one endothermic peaks at 168, 274, and 418 °C, respectively. The PXRD patterns also show that the coordination framework tends to collapse at 200–250 °C.

Photoluminescence Properties. Polymeric silver(I) coordination complexes with aromatic ligands have received much attention for the development of hybrid luminescent materials.^{5,25} Thus, solid-state fluorescent properties of complexes **1–5** were explored at room temperature. The excitation and emission spectra of **1–5** and bpe are shown in Figure S3 and Figure 6. The free bpe ligand shows the maximal emission peak at 497 nm ($\lambda_{\text{ex}} = 340$ nm), which can be ascribed to the $\pi \rightarrow \pi^*$ and/or $n \rightarrow \pi^*$ transitions. Excitation of the microcrystalline samples of **1–5** leads to the generation of similar fluorescent emissions, with the peak maxima occurring at 493 nm (for **1** and **2**) and 494 nm (for **3–5**). Obviously, these emission peaks should come from the ligand-centered transitions, and the slight redshift compared to that of bpe may result from the effect of metal–ligand coordination interactions. Moreover, visible enhancement of their emission intensity in comparison with that of the free ligand may be attributed to the increased rigidity of bpe when bound to the Ag⁺ center, which will effectively reduce the loss of energy.²⁶

Conclusions and Perspective

This work presents five novel silver(I) coordination polymers based on the bpe spacer and a series of *R*-benzenedicarboxyl tectons (*R* = -H, -SO₃H, -NH₂, and -Br), showing a variety of network architectures such as the 3-D (10,3)-*b* framework, 2-D (4.6)²(4³.6².8)(4⁴.6⁰) and 6³ layers, and complicated 3-D 8-nodal self-penetrating network. These interesting structures are essentially regulated by the diversified bridging fashions of the dicarboxylate building blocks and the adaptable coordination spheres of silver(I). The significant substituent effect for such dicarboxylate ligands has also been demonstrated to rationally modify the resulting polymeric networks. In addition, such coordination polymers display modest thermal stability and strong solid-state fluorescent emission. Accordingly, these results may offer new insights into crystal engineering of coordination crystalline materials, and further systematic investigations of the substituent effect for organic tectons on structural construction of related supramolecular systems are ongoing.

Acknowledgment. This work was financially supported by the National Natural Science Foundation of China (20671071 and 20971098), Program for New Century Excellent Talents in University (NCET-07-0613), Tianjin Normal University, and SRF for ROCS, SEM.

Supporting Information Available: Crystallographic data in CIF format, powder X-ray diffraction (PXRD) patterns, fluorescent excitation spectra in the solid state, selected bond parameters and possible hydrogen-bonding geometries. This material is available free of charge via the Internet at <http://pubs.acs.org>.

References

- (1) For related reviews, see (a) Khlobystov, A. N.; Blake, A. J.; Champness, N. R.; Lemenovskii, D. A.; Majouga, A. G.; Zykl, N. V.; Schröder, M. *Coord. Chem. Rev.* **2001**, 222, 155. (b) Zheng, S.-L.; Tong, M.-L.; Chen, X.-M. *Coord. Chem. Rev.* **2003**, 246, 185. (c) Chen, C.-L.; Kang, B.-S.; Su, C.-Y. *Aust. J. Chem.* **2006**, 59, 3. (d) Dorn, T.; Fromm, K. M.; Janiak, C. *Aust. J. Chem.* **2006**, 59, 22. (e) Mak, T. C. W.; Zhao, X.-L.; Wang, Q.-M.; Guo, G.-C. *Coord. Chem. Rev.* **2007**, 251, 2311. (f) Steel, P. J.; Fitchett, C. M. *Coord. Chem. Rev.* **2008**, 252, 990. (g) Young, A. G.; Hanton, L. R. *Coord. Chem. Rev.* **2008**, 252, 1346. (h) Meijboom, R.; Bowen, R. J.; Berners-Price, S. J. *Coord. Chem. Rev.* **2009**, 253, 325.

- (2) (a) Carlucci, L.; Ciani, G.; Proserpio, D. M. *Chem. Commun.* **1999**, 449. (b) Blake, A. J.; Champness, N. R.; Howdle, S. M.; Webb, P. B. *Inorg. Chem.* **2000**, 39, 1035. (c) Bu, X.-H.; Liu, H.; Du, M.; Wong, K. M. C.; Yam, V. W. W.; Shionoya, M. *Inorg. Chem.* **2001**, 40, 4143. (d) Brandys, M. C.; Puddephatt, R. J. *Chem. Commun.* **2001**, 1508. (e) Sun, D.-F.; Cao, R.; Sun, Y.-Q.; Bi, W.-H.; Li, X.-J.; Wang, Y.-Q.; Shi, Q.; Li, X. *Inorg. Chem.* **2003**, 42, 7512. (f) Tong, M.-L.; Wu, Y.-M.; Ru, J.; Chen, X.-M.; Chang, H.-C.; Kitagawa, S. *Inorg. Chem.* **2002**, 41, 4846. (g) Du, M.; Zhao, X.-J.; Guo, J.-H.; Batten, S. R. *Chem. Commun.* **2005**, 4836. (h) Bourlier, J.; Jouaiti, A.; Kyritsakas-Gruber, N.; Allouche, L.; Planeix, J. M.; Hosseini, M. W. *Chem. Commun.* **2008**, 6191. (i) Reger, D. L.; Foley, E. A.; Smith, M. D. *Inorg. Chem.* **2009**, 48, 936. (j) Zhao, L.; Mak, T. C. W. *Inorg. Chem.* **2009**, 48, 6480.
- (3) (a) Hoffart, D. J.; Dalrymple, S. A.; Shimizu, G. K. H. *Inorg. Chem.* **2005**, 44, 8868. (b) Kuroda-Sowa, T.; Liu, S.-Q.; Yamazaki, Y.; Munakata, M.; Maekawa, M.; Suenaga, Y.; Konaka, H.; Nakagawa, H. *Inorg. Chem.* **2005**, 44, 1686. (c) Uchida, S.; Kawamoto, R.; Tagami, H.; Nakagawa, Y.; Mizuno, N. *J. Am. Chem. Soc.* **2008**, 130, 12370. (d) Zhang, J.-P.; Kitagawa, S. *J. Am. Chem. Soc.* **2008**, 130, 907.
- (4) (a) Kascatan-Nebioglu, A.; Panzner, M. J.; Tessier, C. A.; Cannon, C. L.; Youngs, W. J. *Coord. Chem. Rev.* **2007**, 251, 884. (b) Kasuga, N. C.; Sugie, A.; Nomiya, K. *Dalton Trans.* **2004**, 3732.
- (5) (a) Wu, C.-D.; Ngo, H. L.; Lin, W. *Chem. Commun.* **2004**, 1588. (b) Seward, C.; Jia, W.-L.; Wang, R.-Y.; Enright, G. D.; Wang, S. *Angew. Chem., Int. Ed.* **2004**, 43, 2933. (c) Lin, P.; Henderson, R. A.; Harrington, R. W.; Clegg, W.; Wu, C.-D.; Wu, X.-T. *Inorg. Chem.* **2004**, 43, 181. (d) Catalano, V. J.; Moore, A. L. *Inorg. Chem.* **2005**, 44, 6558. (e) Liu, S.-Q.; Kuroda-Sowa, T.; Konaka, H.; Suenaga, Y.; Maekawa, M.; Mizutani, T.; Ning, G.-L.; Munakata, M. *Inorg. Chem.* **2005**, 44, 1031. (f) Chen, Y.-S.; Tal, A.; Torrance, D. B.; Kuebler, S. M. *Adv. Funct. Mater.* **2006**, 16, 1739. (g) Fernandez-Fernandez, M. D.; Bastida, R.; Macias, A.; Perez-Lourido, P.; Valencia, L. *Inorg. Chem.* **2006**, 45, 2266. (h) Liu, X.; Guo, G.-C.; Fu, M.-L.; Liu, X.-H.; Wang, M.-S.; Huang, J.-S. *Inorg. Chem.* **2006**, 45, 3679. (i) Zhang, S.-M.; Hu, T.-L.; Li, J.-R.; Du, J.-L.; Bu, X.-H. *CrystEngComm* **2008**, 10, 1595.
- (6) (a) Coleman, K. S.; Chamberlayne, H. T.; Turberville, S.; Green, M. L. H.; Cowley, A. R. *Dalton Trans.* **2003**, 2917. (b) Samantaray, M. K.; Katiyar, V.; Roy, D.; Pang, K. L.; Nanavati, H.; Stephen, R.; Sunoj, R. B.; Ghosh, P. *Eur. J. Inorg. Chem.* **2006**, 2975. (c) Willans, C. E.; Anderson, K. M.; Junk, P. C.; Barbour, L. J.; Steed, J. W. *Chem. Commun.* **2007**, 3634. (d) Fujii, Y.; Terao, J.; Kambe, N. *Chem. Commun.* **2009**, 1115.
- (7) (a) Zhang, D.-Q.; Ding, L.; Xu, W.; Hu, H.-M.; Zhu, D.-B.; Huang, Y.-H.; Fang, D.-C. *Chem. Commun.* **2002**, 44. (b) Yamada, S.; Ishida, T.; Nogami, T. *Dalton Trans.* **2004**, 898.
- (8) (a) Su, C.-Y.; Cai, Y.-P.; Chen, C.-L.; Smith, M. D.; Kaim, W.; zur Loye, H.-C. *J. Am. Chem. Soc.* **2003**, 125, 8595. (b) Dias, H. V. R.; Singh, S. *Inorg. Chem.* **2004**, 43, 7396.
- (9) (a) Burchell, T. J.; Puddephatt, R. J. *Inorg. Chem.* **2006**, 45, 650. (b) Zhao, L.; Mak, T. C. W. *J. Am. Chem. Soc.* **2005**, 127, 14966. (c) Wu, H.; Dong, X.-W.; Liu, H.-Y.; Ma, J.-F.; Li, S.-L.; Yang, J.; Liu, Y.-Y.; Su, Z.-M. *Dalton Trans.* **2008**, 5331.
- (10) (a) Sumby, C. J.; Gordon, K. C.; Walsh, T. J.; Hardie, M. J. *Chem.—Eur. J.* **2008**, 14, 4415. (b) Du, J.-L.; Hu, T.-L.; Zhang, S.-M.; Zeng, Y.-F.; Bu, X.-H. *CrystEngComm* **2008**, 10, 1866. (c) Lu, J.; Xiao, F.-X.; Shi, L.-X.; Cao, R. J. *Solid State Chem.* **2008**, 181, 313.
- (11) (a) Zheng, S.-L.; Tong, M.-L.; Yu, X.-L.; Chen, X.-M. *J. Chem. Soc., Dalton Trans.* **2001**, 586. (b) Schultheiss, N.; Powell, D. R.; Bosch, E. *Inorg. Chem.* **2003**, 42, 5304. (c) Zang, S.-Q.; Mak, T. C. W. *Inorg. Chem.* **2008**, 47, 7094.
- (12) (a) Carlucci, L.; Ciani, G.; Proserpio, D. M.; Porta, F. *CrystEngComm* **2006**, 8, 696. (b) Sun, Q.-Z.; Wei, M.-L.; Bai, Y.; He, C.; Meng, Q.-J.; Duan, C.-Y. *Dalton Trans.* **2007**, 4089. (c) Du, M.; Li, C.-P.; Guo, J.-H. *CrystEngComm* **2009**, 11, 1536.
- (13) Du, M.; Bu, X.-H. In *Design and Construction of Coordination Polymers*; Hong, M.-C.; Chen, L., Ed.; John Wiley: New York, 2009; Chapter 6, pp 145–170.
- (14) (a) Li, C.-P.; Tian, Y.-L.; Guo, Y.-M. *Inorg. Chem. Commun.* **2008**, 11, 1405. (b) Li, C.-P.; Tian, Y.-L.; Guo, Y.-M. *Polyhedron* **2009**, 28, 505. (c) Du, M.; Zhang, Z.-H.; You, Y.-P.; Zhao, X.-J. *CrystEngComm* **2008**, 10, 306. (d) Li, C.-P.; Chen, J.; Du, M. *Polyhedron* **2010**, 29, 463.
- (15) (a) Li, C.-P.; Yu, Q.; Du, M. *Sci. China Ser. B-Chem.* **2009**, 52, 1470. (b) Li, C.-P.; Yu, Q.; Zhang, Z.-H.; Du, M. *CrystEngComm* **2010**, 12, 834. (c) Yu, Q.; Li, C.-P.; Zhang, Z.-H.; Du, M. *Polyhedron* **2009**, 28, 2347. (d) Du, M.; Li, C.-P.; Zhao, X.-J. *CrystEngComm* **2006**, 8, 552.
- (16) (a) SAINT Software Reference Manual; Bruker AXS: Madison, WI, 1998. (b) Sheldrick, G. M. *SHELXTL NT Version 5.1. Program for Solution and Refinement of Crystal Structures*; University of Göttingen: Göttingen, Germany, 1997.
- (17) Janiak, C. *J. Chem. Soc., Dalton Trans.* **2000**, 3885.
- (18) For interpretation of the three-letter net codes, see Ockwig, N. W.; Delgado-Friedrichs, O.; O'Keeffe, M.; Yaghi, O. M. *Acc. Chem. Res.* **2005**, 38, 176 and the associated website <http://rCSR.anu.edu.au/>.
- (19) Venkataraman, D.; Du, Y.; Wilson, S. R.; Hirsch, K. A.; Zhang, P.; Moore, J. S. *J. Chem. Educ.* **1997**, 74, 915.
- (20) All topological calculations were made by using the *TOPOS* package, see Blatov, V. A. *TOPOS, A Multipurpose Crystallochemical Analysis with the Program Package*; Samara State University: Russia, 2004.
- (21) Addison, A. W.; Rao, T. N.; Reedijk, J.; van Rijn, J.; Verschoor, G. C. *J. Chem. Soc., Dalton Trans.* **1984**, 1349.
- (22) (a) Rarig, R. S., Jr.; Zubietta, J. *Inorg. Chim. Acta* **2001**, 319, 235. (b) Zhong, K.-L.; Lu, W.-J. *Acta Crystallogr.* **2005**, E61, m1416.
- (23) For the dihedral angles of two coordinated pyridyl rings in bpe, the corresponding values in the known examples are 40.4(2)/32.1(2), 50.6(1)/56.5(1), 27.7(2), 3.8(1)/11.0(1), and 6.3(1)/11.2(1)°, respectively.
- (24) Hill, Y.; Briceño, A. *Chem. Commun.* **2007**, 3930.
- (25) Allendorf, M. D.; Bauer, C. A.; Bhakta, R. K.; Houk, R. J. T. *Chem. Soc. Rev.* **2009**, 38, 1330.
- (26) (a) Yi, L.; Zhu, L.-N.; Ding, B.; Cheng, P.; Liao, D.-Z.; Yan, S.-P.; Jiang, Z.-H. *Inorg. Chem. Commun.* **2003**, 6, 1209. (b) Cai, L.-Z.; Chen, W.-T.; Wang, M.-S.; Guo, G.-C.; Huang, J.-S. *Inorg. Chem. Commun.* **2004**, 7, 611.